Scientific Journals
of the Maritime University of Szczecin

Zeszyty Naukowe
Akademii Morskiej w Szczecinie

2018, 54 (126), 35–43
ISSN 1733-8670 (Printed)
ISSN 2392-0378 (Online)
DOI: 10.17402/283

Received: 15.03.2018
Accepted: 24.05.2018
Published: 15.06.2018

Parameters affecting water hammer in plastic pipelines

Kamil Urbanowicz, Mateusz Firkowski

West Pomeranian University of Technology Szczecin
Department of Mechanical Engineering and Mechatronics
19 Piastów Ave., 70-310 Szczecin, Poland
e-mail: {kamil.urbanowicz; mateusz.firkowski}@zut.edu.pl
corresponding author

Key words: water hammer, unsteady flow, viscoelastic pipes, method of characteristics, partial differential equations, creep function

Abstract
Pressure pipes made of selected plastics are widely used in current water supply systems. Unfortunately, the theoretical basis for modeling transient flows in these pipes has not been clarified yet. For simplified one-dimensional numerical modeling, a model is commonly used in which the total deformation of the pipe walls is expressed by the sum of instantaneous and retarded deformations. One of the main problems lies in the correct experimental determination of the creep function defining the properties of the polymer. The influence of other parameters on which the numerical solution of the method of characteristics is based is the subject of the research presented in this paper.

Introduction

Pipes of plastic (PP, PE, PVC, PB and ABS) have been widely used in engineering practice for many years. The majority of newly designed water supply networks, home connections and internal installations supplying households with water are systems based on polypropylene (PP), polyethylene (PE) or polyvinyl chloride (RPVC). Modern air-conditioning systems, which distribute refrigerants in the form of glycol or chilled water, are often based on plastic conduit made of acrylonitrile butadiene styrene (ABS). This material retains its mechanical properties at temperatures as low as −40°C. However, in central heating installations, polybutylene (PB) pipes can be used, which are adapted to higher temperatures of the working medium.

A feature that distinguishes plastic pipes from pipes made of other materials is their viscoelasticity (Covas et al., 2004; Urbanowicz, Firkowski & Zarzycki, 2016). The modulus of elasticity is a function of time and temperature, which is determined experimentally. The unsteady flows in these pipelines may be accompanied by all the other phenomena that occur in systems of classic conduits, i.e., cavitation (Bergant, Simpson & Tijsseling, 2006; Zarzycki & Urbanowicz, 2006; Adamkowski & Lewandowski, 2012), friction (Zarzycki, 1997, 2000; Vardy & Brown, 2003, 2004; Urbanowicz, 2017a) and fluid structure interaction (FSI) (Tijsseling, 2007; Perotti et al., 2013; Henclik, 2018a, 2018b).

Occurrence of a severe water hammer in hydraulic systems installed on ships (hydraulic systems for steering gear, pitch propellers, watertight doors, cargo hatch covers, cargo and mooring winches, deck cranes, stern ramps etc.) is not acceptable (Urbanowicz, 2017a). It is almost always associated with the occurrence of minor or major damage. Repairing the damage at sea is often impossible due to the lack of spare parts and, if done temporarily, it can quickly prevent the further safe travel of the ship. This paper will examine the effect of parameters that occur in the basic equations describing unsteady flow in these viscoelastic pipes, by omitting the influence of cavitation and FSI. The acquired knowledge will in the

future better optimize hydraulic systems of this type at the design stage.

Basic equations

Basic equations describing transient flow in viscoelastic pipes are respectively equations of continuity and motion (Urbanowicz, Firkowski & Zarzycki, 2016):

$$\begin{cases} \dfrac{1}{\rho c^2}\dfrac{\partial p}{\partial t}+\dfrac{\partial v}{\partial x}+\Xi\displaystyle\int_0^t \frac{\partial p(u)}{\partial t}\cdot w_J(t-u)\,\mathrm{d}u=0 \\ \rho\dfrac{\partial v}{\partial t}+\dfrac{\partial p}{\partial x}+\dfrac{2\rho}{R}\left(\dfrac{v|v|}{8}f+\dfrac{2v}{R}\displaystyle\int_0^t \frac{\partial v}{\partial t}(u)\cdot w(t-u)\,\mathrm{d}u\right)=0 \end{cases} \tag{1}$$

where:

p – pressure [Pa];
v – mean cross section velocity [m/s];
t – time [s];
x – distance along the pipe [m];
ρ – liquid density [kg/m^3];
c – pressure wave speed [m/s];
R – inner pipe radius [m];
f – friction coefficient [–];
v – kinematic viscosity [m^2/s];
$w\,(t-u)$ – weighting function [–];
$w_J\,(t-u)$ – time derivative of pipe material creep compliance function [s^{-1}Pa^{-1}].

In single-phase flow, the velocity of pressure wave propagation is a function of six parameters $c = f(\rho, K, v_P, R, J_0, e)$, given by:

$$c=\sqrt{\frac{1}{\rho\left[\dfrac{1}{K}+\Xi\,J_0\right]}} \tag{2}$$

where:

$\Xi = 2\dfrac{R}{e}\alpha$ – enhanced α parameter [–];
K – liquid bulk modulus [Pa];
J_0 – instantaneous component of creep [Pa^{-1}];
e – thickness of pipe wall [m];
α – parameter describing support condition of pipe [–]:

$$\alpha=\frac{2e}{D}(1+v_P)+\frac{D}{D+e}\left(1-v_P^2\right) \tag{3}$$

Some of these parameters of the water hammer model appear only in the formula for the propagation velocity of the pressure wave; they are K and $J_0 = 1/E_0$. Friction factor and the parameter describing the support condition of pipe α in this work are modelled as in Urbanowicz (2017b). With the method of characteristics used for an inner grid node, the numerical solution of the set of partial derivative equations (2) is:

$$p_{i,t+\Delta t}=\frac{C_{i-1,t}-C_{i+1,t}}{\dfrac{2}{\rho c}+4c\,\Delta t\,F},\quad v_{i,t+\Delta t}=\frac{C_{i-1,t}+C_{i+1,t}}{2} \tag{4}$$

where

$$\begin{cases} C_{i-1,t}=v_{i-1,t}+\dfrac{p_{i-1,t}}{\rho c}-\dfrac{2\Delta t}{\rho R}\tau_{i-1,t}+2c\Delta t I_{i,t} \\ C_{i+1,t}=v_{i+1,t}-\dfrac{p_{i+1,t}}{\rho c}-\dfrac{2\Delta t}{\rho R}\tau_{i+1,t}-2c\Delta t I_{i,t} \end{cases} \tag{5}$$

$$I_{i,t}=\frac{1}{2}\Xi\sum_{j=1}^{n}\left(F_j p_{i,t}-x_{j,t}G_j\right) \tag{6}$$

and

$$F_j=\frac{J_j}{\Delta t}\left[1-e^{-\frac{\Delta t}{T_j}}\right],\quad G_j=e^{-\frac{\Delta t}{T_j}} \tag{7}$$

$$F=\frac{1}{2}\Xi\sum_{j=1}^{n}F_j \tag{8}$$

After calculating the actual value of pressure, it is needed to calculate the time dependent x_j coefficient (which for an initial steady flow has a zero value):

$$x_{j,t+\Delta t}=x_{j,t}G_j+\left(p_{j,t+\Delta t}-p_{i,t}\right)F_j \tag{9}$$

The wall shear stress τ is calculated from the corrected efficient convolution integral solution (Urbanowicz, 2015; Urbanowicz & Zarzycki, 2015). The coefficients m_j and n_j that represent the weighting function are calculated using an analytical solution presented in recent work (Urbanowicz, 2017b), which were based on the calculation algorithm presented at the 11th International Conference on Pressure Surges (Urbanowicz, 2012).

Roles of parameters

This section is devoted to analysis of the impact of individual parameters occurring in the equations discussed in the previous section, which have an effect on simulated transient flows in plastic conduits. The initial values of the tested parameters (Table 1 – the second column) were adopted using experimental studies carried out at Imperial College of London by Covas et al. (Covas et al., 2005). The analyzed experimental setup had a pipe of high-density polyethylene SDR11 PE100 NP16, with a length L = 271.7 m. From the analysis of observed experimental dynamic courses of pressure changes, the actual velocity of propagation of the pressure wave in the tested system

a) laminar case

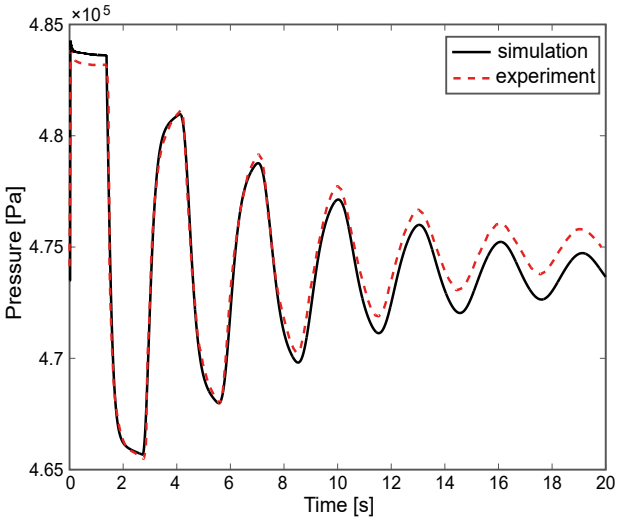

b) turbulent case

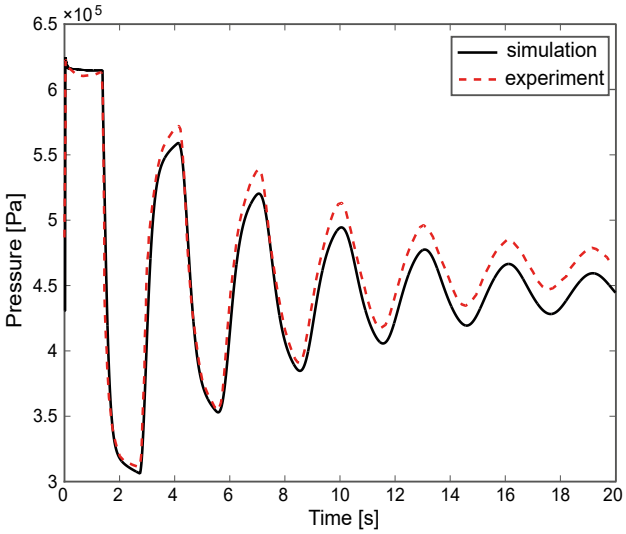

Figure 1. Fit of simulation results for initial values of tested parameters given in Table 1

Table 1. Initial, minimal and maximal values of water hammer parameters

Parameter	Initial parameters	Assumed deviation	Minimal value	Maximal value
ρ [kg/m^3]	998.2	±5%	$\rho_1 = 948$	$\rho_2 = 1048$
R [m]	0.0253	±5%	$R_1 = 0.024035$	$R_2 = 0.026565$
e [m]	0.0063	±5%	$e_1 = 0.005985$	$e_2 = 0.006615$
ν_P [–]	0.46	±10%	$\nu_{P1} = 0.414$	$\nu_{P2} = 0.506$
ν [m^2/s]	$1 \cdot 10^{-6}$	±10%	$\nu_1 = 0.9 \cdot 10^{-6}$	$\nu_2 = 1.1 \cdot 10^{-6}$
K [Pa]	$2 \cdot 10^9$	±10%	$K_1 = 1.8 \cdot 10^9$	$K_2 = 2.2 \cdot 10^9$
J_0 [Pa^{-1}]	$0.674 \cdot 10^{-9}$	±10%	$J_{01} = 0.607 \cdot 10^{-9}$	$J_{02} = 0.741 \cdot 10^{-9}$

was determined at $c = 400$ m/s. For this value of speed, while maintaining the other parameters (Table 1 – the second column) and using the numerical division of the pipe into the selected number $N = 64$ of sections, a good correspondence of the simulated pressure runs was obtained (laminar flow $v_0 = 0.031$ m/s and turbulent flow $v_0 = 0.455$ m/s) with experimental observed runs, which is confirmed by graphical comparisons – see Figure 1.

The results of the numerical simulations carried out, which show the impact of individual parameters, are presented in Figures 2, 3 and 4. From all the analyzed parameters only the kinematic viscosity ν does not affect the value of pressure wave propagation. The exact influence of the adopted parameters on the values of speed c and selected parameters (R, e, and ν_P) on the reported support condition of pipe α and on the enhanced α that is denoted by Ξ is shown in Table 2.

The bulk modulus K for liquids varies with pressure and temperature. It's challenging, even in the case of water, to find in the literature an accurate

Table 2. Dependence of pressure wave speed

Parameter	c [m/s]	Parameter	c [m/s]	Ξ [–]	α [–]
ρ_1	410.38	R_1	406.83	8.24	1.08
ρ_2	390.31	R_2	393.36	8.86	1.05
K_1	398.17	e_1	393.03	8.88	1.05
K_2	401.39	e_2	406.49	8.25	1.08
J_{01}	419.58	ν_{P1}	395.80	8.75	1.09
J_{02}	382.81	ν_{P2}	404.87	8.33	1.04

solution, from which one can calculate K for different temperature and pressure. The change of this parameter only slightly affects Table 2 in calculations of the predicted value of pressure wave speed (Figures 3a and 3b).

Covas (Covas et al., 2004) mentioned the problems associated with getting the exact value of the instantaneous component of creep J_0, which is the inverse of Young's modulus of elasticity. This parameter only affects the pressure wave speed value, and as the obtained results, it has a significant impact on its change (Figures 3c and 3d). The density ρ of the

a) laminar case

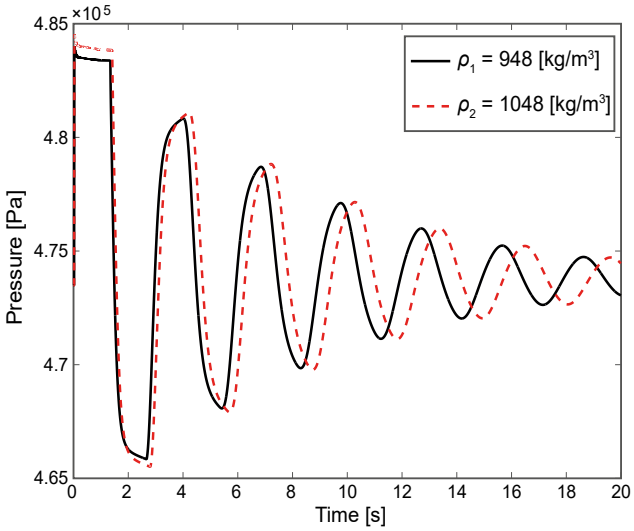

b) turbulent case

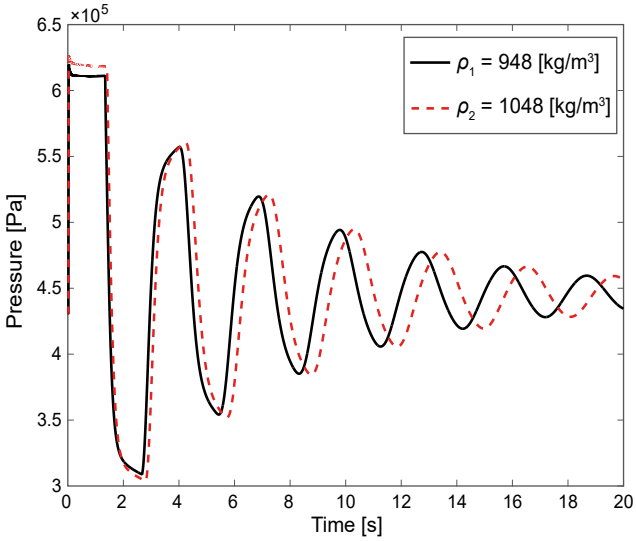

c) laminar case

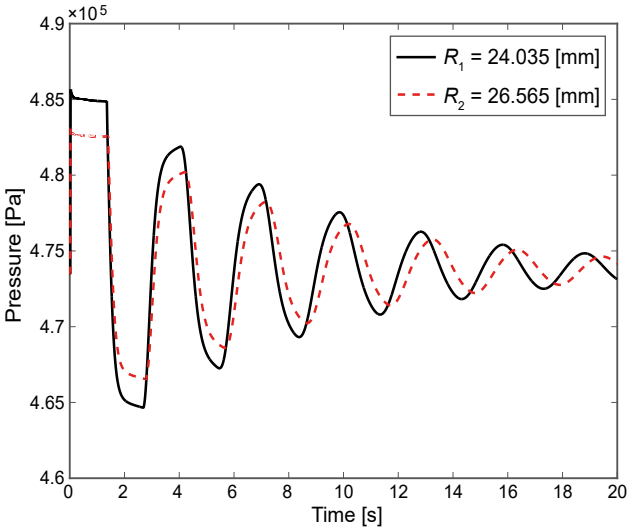

d) turbulent case

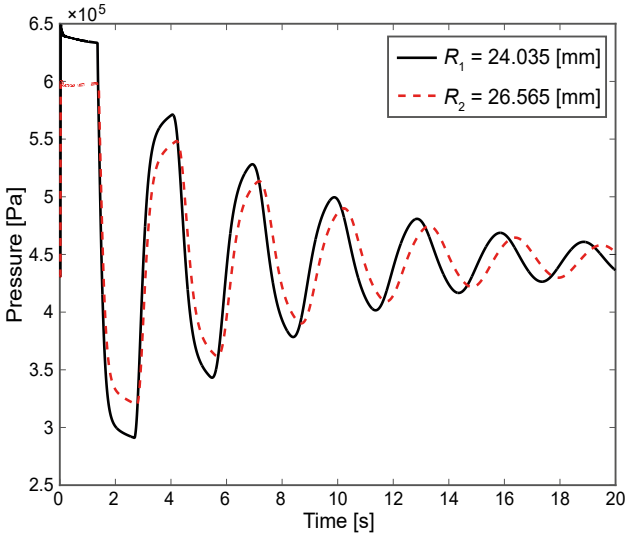

e) laminar case

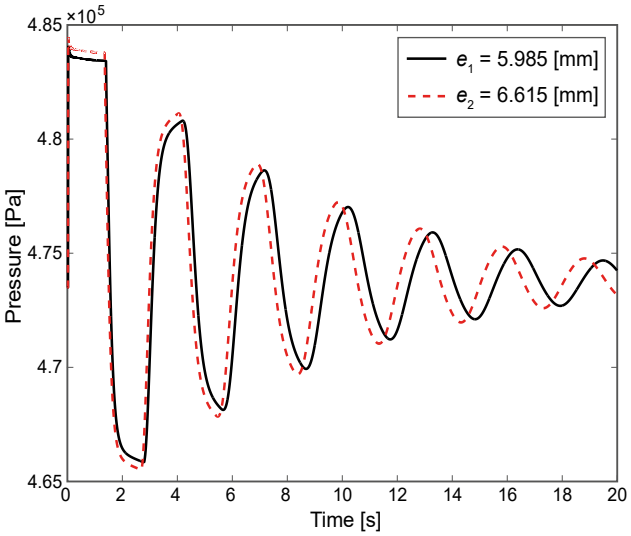

f) turbulent case

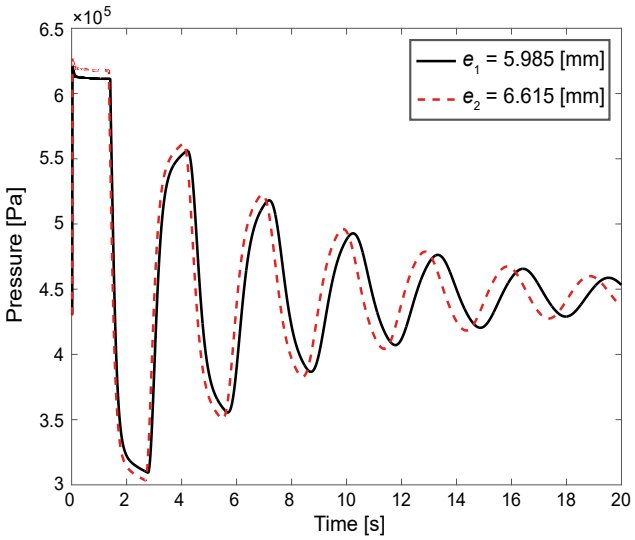

Figure 2. Liquid density ρ, inner pipe radius R and wall thickness e effects (left column: laminar flow results, right column: turbulent flow results)

a) laminar case

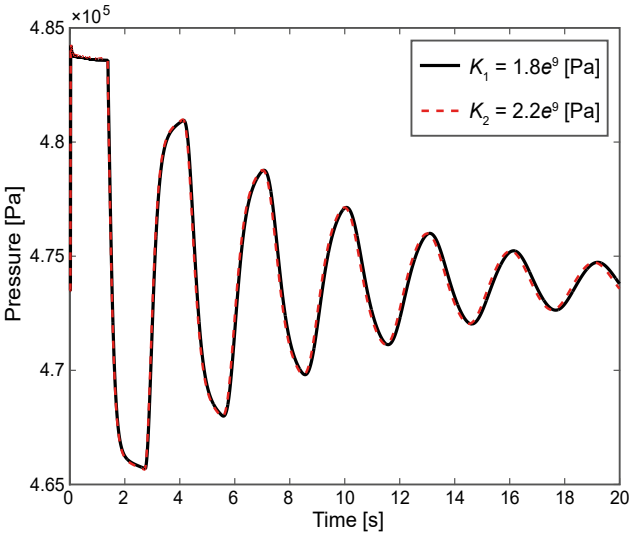

b) turbulent case

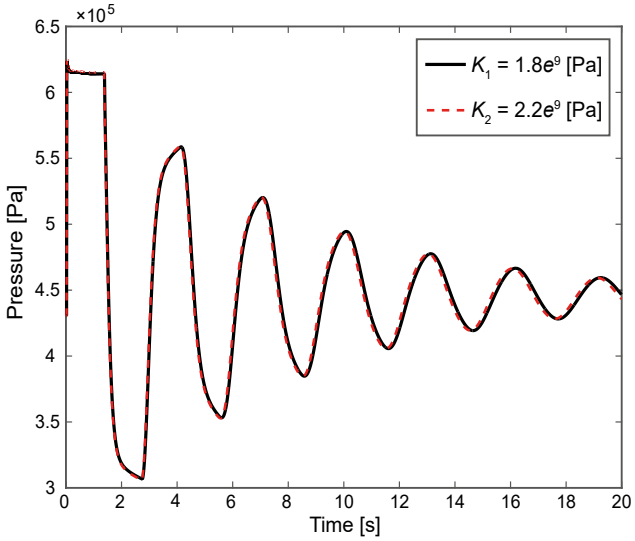

c) laminar case

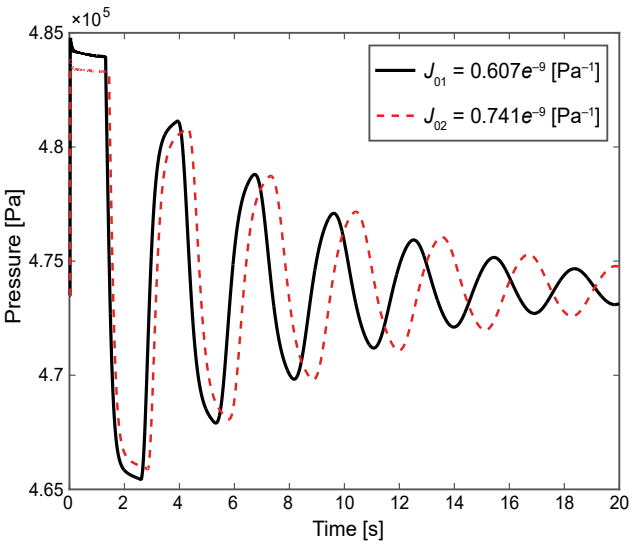

d) turbulent case

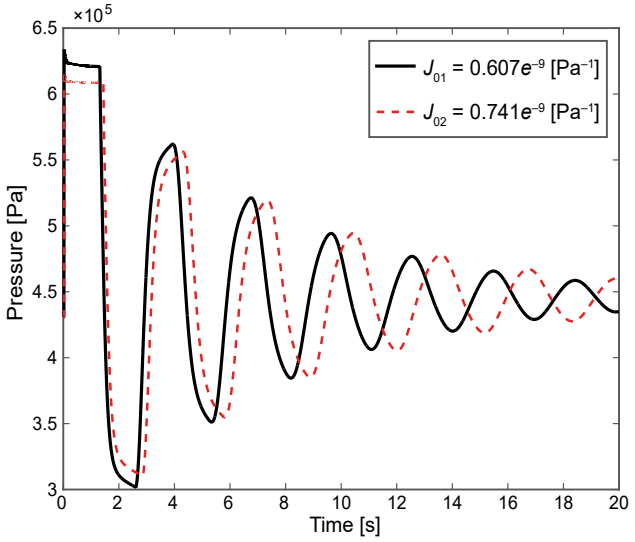

e) laminar case

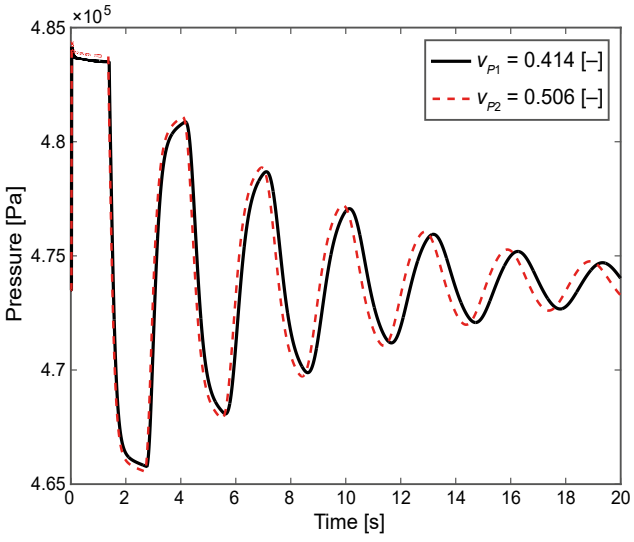

f) turbulent case

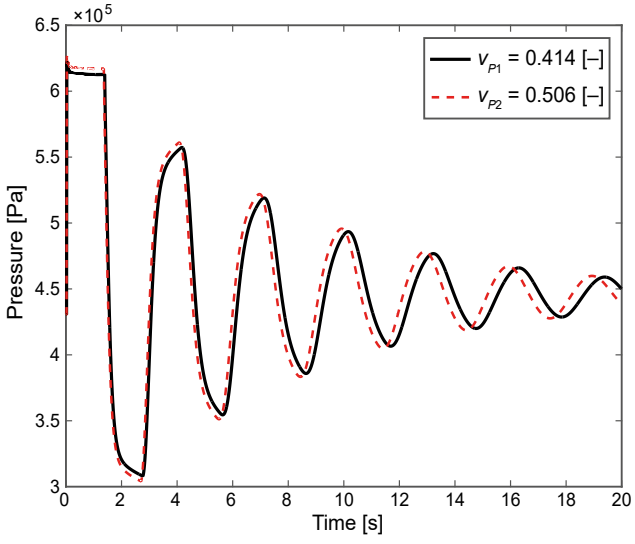

Figure 3. Liquid bulk modulus K, instantaneous component of creep modulus J_0 and Poisson coefficient ν_P effects (left column: laminar flow results, right column: turbulent flow results)

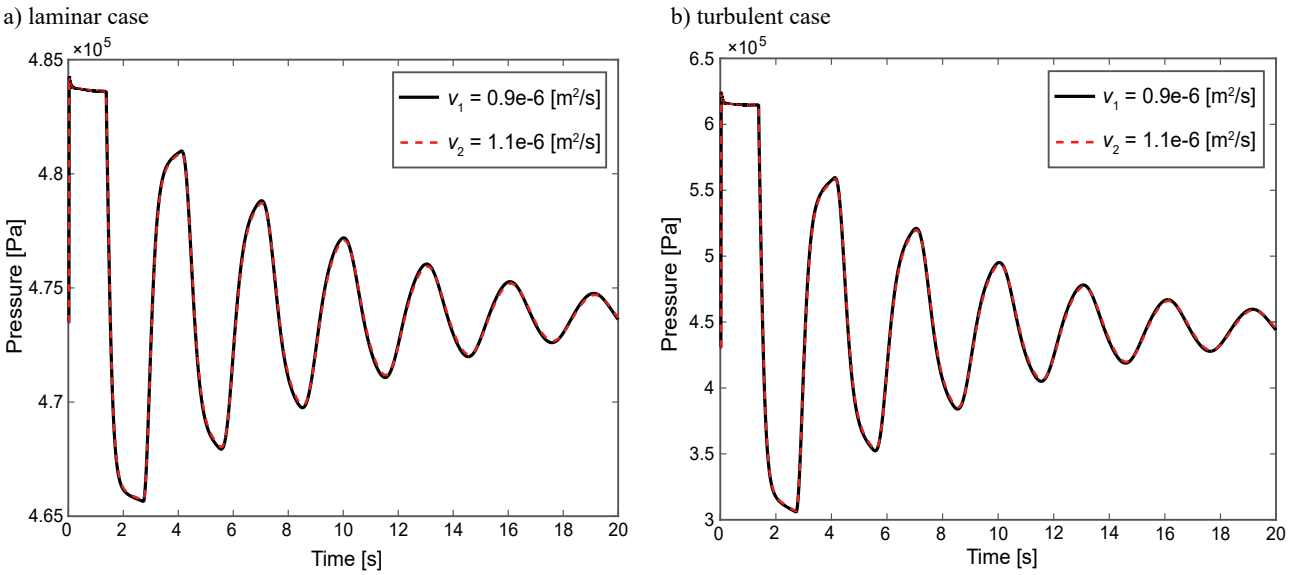

Figure 4. Liquid kinematic viscosity effect

flowing liquid directly influences the results of the simulation through the final equations of the method of characteristics (4) and (5) as well as, indirectly, the pressure wave speed (2). The internal radius of the pipe R affects the pressure wave speed, both explicit and implicit, by modifying the α coefficient, simulated hydraulic resistance and the simulated viscoelastic effect (Figures 2c and 2d). The thickness of the wall e leads to the modification of c in an explicit and implicit manner by the factor α and affects the modelling of the viscoelastic behavior of the pipe wall; however, it does not affect the modelling of hydraulic resistance (Figures 2e and 2f). The last parameter that influences the pressure wave speed, although indirectly by the factor α, is Poisson's ratio ν_P (Figures 3e and 3f).

The coefficient of kinematic viscosity determines the value of the modelled instantaneous wall shear stress but does not affect the value of the pressure wave speed (Figure 4), nor directly the terms of the numerical solution (4). However, the adopted change in viscosity in the range of ±10% (simulations presented on Figure 4) does not reflect the possible change in viscosity as a function of temperature. Sample results for water at a temperature of about 0°C and temperature of about 95°C are shown in Figure 6a. The viscosity of some hydraulic oils changes even more rapidly as a function of temperature, therefore the effect of temperature of the flowing liquid should always be taken into account when computing the approximate value of viscosity.

The effect of physical parameters on seventh amplitude delays T_7, first p_1 and seventh amplitude p_7 pressure increase, are presented in Table 3. The following arrows mean: ↑ – large increase, ↓ – large decrease, ↗ – small increase, ↘ – small decrease, ↔ – unnoticeable change.

Table 3. Single parameter tendencies

when: ↑ of	then p_1	and p_7	and T_7
ρ	↑	↘	↑
R	↓	↓	↑
e	↑	↑	↓
ν_P	↑	↗	↓
ν	↔	↔	↔
K	↗	↘	↘
J_0	↓	↑	↑

Let us now consider the effect on the simulations of an increase or decrease at one time of three parameters: R, e and ν_P. The dimensionless coefficient α (3) is determined using these parameters and, next, the enhanced α parameter Ξ. These parameters influence the numerical results of calculations of convolutional integrals (1), as well as the values of pressure wave speed c (2).

The trends obtained are summarized in Table 4, while the simulation results are shown in Figures 5a and 5b. Assuming $\nu_{P2} = 0.506$, $R_1 = 0.024035$

Table 4. Analysis of changes in the Ξ parameter

Ξ_{min}		Ξ_{max}	
when	then	when	then
ν_P ↑	Ξ ↓	ν_P ↓	Ξ ↑
R ↓	Ξ ↓	R ↑	Ξ ↑
e ↑	Ξ ↓	e ↓	Ξ ↑

and e_2 = 0.006615, the calculated Ξ = 7.764 and c_{max} = 418.02 m/s; the opposite situation took place for ν_{P1} = 0.414, R_2 = 0.026565 and e_1 = 0.005985, then calculated Ξ = 9.439 and c_{min} = 382.09 m/s.

Keramat and Haghighi (Keramat & Haghighi, 2014) mentioned the possibility of determining the α coefficient using a different formula:

$$\alpha = \left(1-\nu^2\right)+\alpha_r \nu \left(1+\nu\right)\frac{2e}{D} \tag{10}$$

where: α_r – averaging factor (1/2 according to Rachid and Stuckenbruck (Rachid & Stuckenbruck, 1990) and 3/4 according to Tijsseling (Tijsseling, 2007)). If one calculates α (Ξ_{min} = 6.168; Ξ_{max} = 7.941) coefficient which relates to the anchors' action using α_r = ½, then the final value for c in this case will be $c_{min} \approx 415$ m/s and $c_{max} \approx 465$ m/s and the graphical representation of the numerical solution is as presented on Figure 6b.

The extreme multi-parameter case occurs when we take into account changes in all parameters, so that the maximum increase or decrease in the pressure wave occurs (Figures 5c and 5d).

Table 5. Tendencies in the extreme case

c_{min}		c_{max}	
when	then	when	then
$J_0 \uparrow$	$c \downarrow$	$J_0 \downarrow$	$c \uparrow$
$K \downarrow$	$c \downarrow$	$K \uparrow$	$c \uparrow$
$\rho \uparrow$	$c \downarrow$	$\rho \downarrow$	$c \uparrow$
$\Xi \uparrow$	$c \downarrow$	$\Xi \downarrow$	$c \uparrow$

a) laminar case

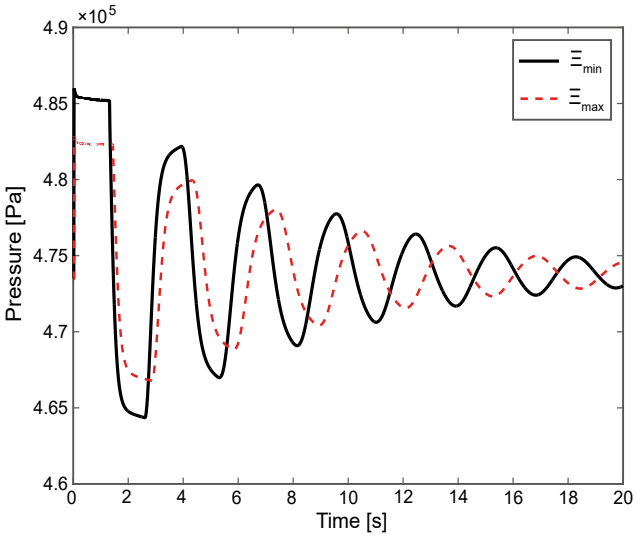

b) turbulent case

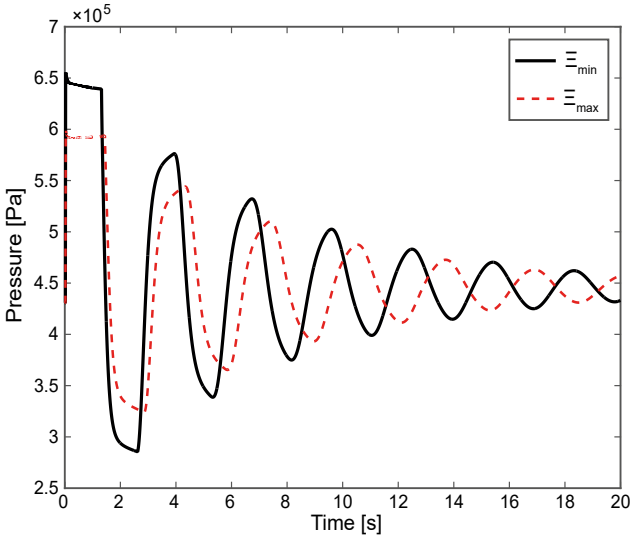

c) laminar case

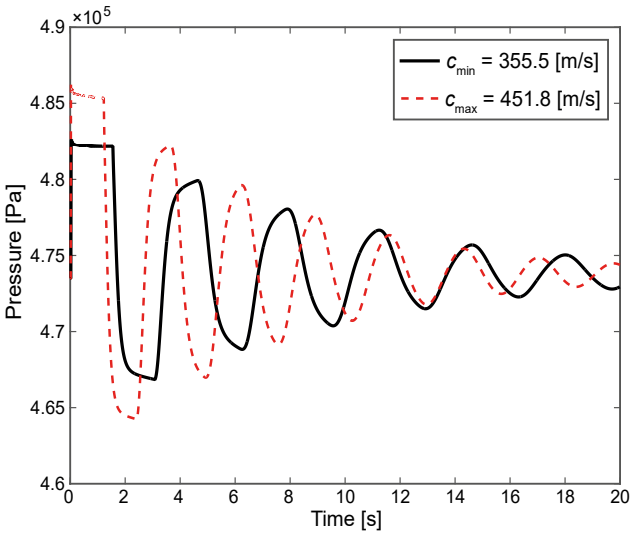

d) turbulent case

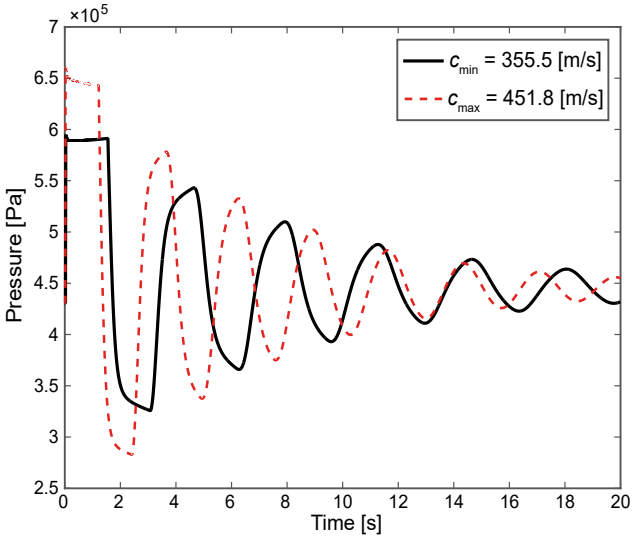

Figure 5. Multi-parameter effects

a) temperature effect on ν of water

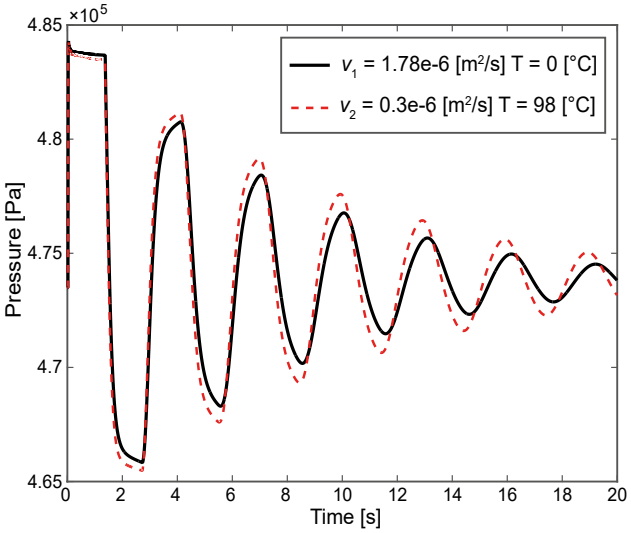

b) Rachid and Stuckenbruck effects

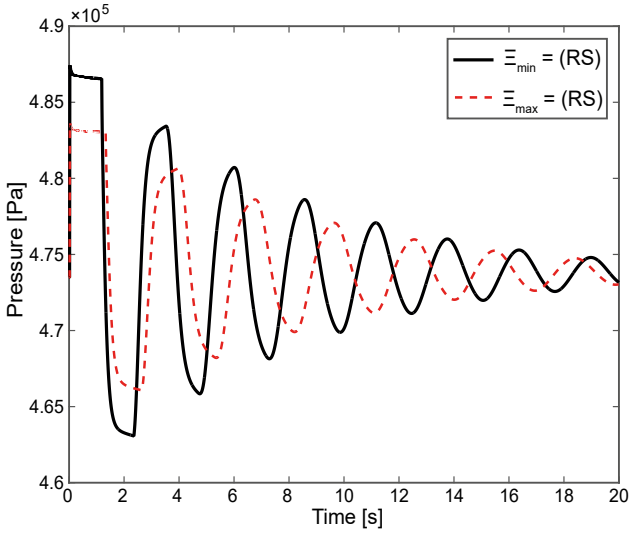

Figure 6. Additional tested effects

The simulation results presented above showed the effect of parameters describing unsteady flow in plastic conduits. As it turned out, the changes in the K coefficient of elasticity and kinematic viscosity have a small influence on the results. On the other hand, the internal radius of the pressure pipe has a very high impact on the maximum pressure increase at the first amplitude. The changes of the Poisson coefficient and the thickness of the pipe wall have a similar effect. The dimensionless parameter Ξ influences the obtained simulation results on a large scale, as it modifies the pressure wave speed and is present in all expressions, being a numerical solution of the convolutional integral describing the influence of the viscoelastic behavior of the material of the pipe walls on the flowing liquid.

Conclusions

The paper shows the influence of numerical method input parameters from the final equations of the characteristics method, on the results of the simulation. If, for water, the determination of the exact density of liquids for a given temperature is not a major question, then for other liquids or water mixtures the situation is much more complicated. It is very difficult to find formulas in textbooks for determining the current value of the bulk modulus (function of temperature and pressure) for water.

The use of different formulas known from the literature for the dimensionless parameter, will significantly affect the results of the simulation. Therefore, further research is recommended, which will allow the correct α formula to be determined, taking into account the influence of the pipe's constraint on the results of the unsteady flow.

In the next stage, after taking into account the models of cavitation, it will be possible to investigate the assumed saturated vapor pressure on the simulated flow.

Acknowledgments

We would like to thank the reviewers for their valuable comments, helpful suggestions and their careful review, which helped to improve the quality of the paper.

References

1. Adamkowski, A. & Lewandowski, M. (2012) Investigation of Hydraulic Transients in a Pipeline with Column Separation. *Journal of Hydraulic Engineering* 138, 11, pp. 935–944.
2. Bergant, A., Simpson, A.R. & Tijsseling, A.S. (2006) Water hammer with column separation: A historical review. *Journal of Fluids and Structures* 22, 2, pp. 135–171.
3. Covas, D., Stoianov, I., Ramos, H., Graham, N. & Maksimovic, C. (2004) The dynamic effect of pipe-wall viscoelasticity in hydraulic transients. Part I – experimental analysis and creep characterization. *Journal of Hydraulic Research* 42, 5, pp. 517–531.
4. Covas, D., Stoianov, I., Ramos, H., Graham, N. & Maksimovic, C. (2005) The dynamic effect of pipe-wall viscoelasticity in hydraulic transients. Part II – model development, calibration and verification. *Journal of Hydraulic Research* 43, 1, pp. 56–70.
5. Henclik, S. (2018a) Analytical solution and numerical study on water hammer in a pipeline closed with an elastically attached valve. *Journal of Sound and Vibration* 417, pp. 245–259.

6. Henclik, S. (2018b) Numerical modeling of water hammer with fluid-structure interaction in a pipeline with viscoelastic supports. *Journal of Fluids and Structures* 76, pp. 469–487.
7. Keramat, A. & Haghighi, A. (2014) Straightforward Transient-Based Approach for the Creep Function Determination in Viscoelastic Pipes. *Journal of Hydraulic Engineering* 140, 12, 04014058.
8. Perotti, L.E., Deiterding, R., Inaba, K., Shepherd, J. & Ortiz, M. (2013) Elastic response of water-filled fiber composite tubes under shock wave loading. *International Journal of Solids and Structures* 50, pp. 473–486.
9. Rachid, F.B.F. & Stuckenbruck, S. (1990) *Transients in liquid and structure in viscoelastic pipes*. Proceedings of the 6th International Conference on Pressure Surges, pp. 69–84.
10. Tijsseling, A.S. (2007) Water hammer with fluid-structure interaction in thick-walled pipes. *Computers & Structures* 85, 11–14, pp. 844–851.
11. Urbanowicz, K. (2012) *New approximation of unsteady friction weighting functions*. Proceedings of the 11th International Conference on Pressure Surges, pp. 477–492.
12. Urbanowicz, K. (2015) *Simple modelling of unsteady friction factor*. Proceedings of the 12th International Conference Pressure Surges, pp. 113–130.
13. Urbanowicz, K. (2017a) Modern Modeling of Water Hammer. *Polish Maritime Research* 24, 3, pp. 68–77.
14. Urbanowicz, K. (2017b) Analytical expressions for effective weighting functions used during simulations of water hammer. *Journal of Theoretical and Applied Mechanics* 55, 3, pp. 1029–1040.
15. Urbanowicz, K., Firkowski, M. & Zarzycki, Z. (2016) Modelling water hammer in viscoelastic pipelines: short brief. *Journal of Physics: Conference Series* 760, 012037.
16. Urbanowicz, K. & Zarzycki, Z. (2015) Improved lumping friction model for liquid pipe flow. *Journal of Theoretical and Applied Mechanics* 53, 2, pp. 295–305.
17. Vardy, A.E. & Brown, J.M.B. (2003) Transient turbulent friction in smooth pipe flows. *Journal of Sound and Vibration* 259, 5, pp. 1011–1036.
18. Vardy, A.E. & Brown, J.M.B. (2004) Transient turbulent friction in fully rough pipe flows. *Journal of Sound and Vibration* 270, 1–2, pp. 233–257.
19. Zarzycki, Z. (1997) *Hydraulic resistance of unsteady turbulent liquid flow in pipes*. Proceedings of the 3rd International Conference on Water Pipeline Systems, pp. 163–178.
20. Zarzycki, Z. (2000) *On weighting function for wall shear stress during unsteady turbulent pipe flow*. Proceedings of the 8th International Conference on Pressure Surges, pp. 529–543.
21. Zarzycki, Z. & Urbanowicz, K. (2006) Modelling of transient flow during water hammer considering cavitation in pressure pipes. *Chemical and Process Engineering* 27, 3, pp. 915–933.